# Direct Observation of Multimer Stabilization in the Mechanical Unfolding Pathway of a Protein Undergoing Oligomerization

Zackary N. Scholl,[*,†] **Weitao Yang,**[‡,†] **and Piotr E. Marszalek**[¶]

[†]Program in Computational Biology and Bioinformatics, Duke University, Durham, North Carolina 27708, United States, [‡]Department of Chemistry, Duke University, Durham, North Carolina 27708, United States, and [¶]Department of Mechanical Engineering and Materials Science, Center for Biologically Inspired Materials and Material Systems, Duke University, Durham, North Carolina 27708, United States

ABSTRACT Understanding how protein oligomerization affects the stability of monomers in self-assembled structures is crucial to the development of new protein-based nanomaterials and protein cages for drug delivery. Here, we use single-molecule force spectroscopy (AFM-SMFS), protein engineering, and computer simulations to evaluate how dimerization and tetramerization affects the stability of the monomer of Streptavidin, a model homotetrameric protein. The

unfolding force directly relates to the folding stability, and we find that monomer of Streptavidin is mechanically stabilized by 40% upon dimerization, and that it is stabilized an additional 24% upon tetramerization. We also find that biotin binding increases stability by another 50% as compared to the apo-tetrameric form. We used the distribution of unfolding forces to extract properties of the underlying energy landscape and found that the distance to the transition state is decreased and the barrier height is increased upon multimerization. Finally, we investigated the origin of the strengthening by ligand binding. We found that, rather than being strengthened through intramolecular contacts, it is strengthened due to the contacts provided by the biotin-binding loop that crosses the interface between the dimers.
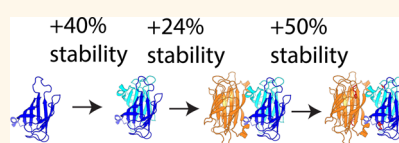
KEYWORDS: protein folding · force spectroscopy · multimerization · simulation

M ultimeric proteins make up 80% of proteomes, although less than 5% of model proteins used in protein folding studies are multimeric.[1] Although it is well-known that the stability of a protein monomer can be drastically affected by its environment, it remains unclear how the process of multimerization influences monomer stability. However, understanding the stability of proteins in the context of their quaternary structure is important for deciphering protein interfaces in viruses[2] and designing new biomaterials[3,4] or drug delivery systems through the use of protein cages.[5] With the use AFM-based single-molecule force-spectroscopy (SMFS, reviewed in ref 6–11), we investigate how multimerization affects the mechanical unfolding pathway of a protein. SMFS allows for the precise characterization of protein (un)folding pathways,[12–25] which are measured along any almost arbitrarily chosen but well-defined reaction coordinate that is consistent with the direction in which the protein is pulled.

Numerous SMFS measurements have also been helpful in determining how ligand binding affects the mechanical stability of proteins[26–29] and have been successfully applied to measure a variety of protein–ligand interactions[30–38] including studies that determined the mechanical strength between oligomer interfaces.[39,40] However, SMFS studies of the stability effects by oligomerizing proteins remain scarce[41,42] though such proteins predominate the proteomes. In a rare recent study, the mechanical effects of aggregation in the intrinsically disordered protein of α-synuclein were examined and found to have mechanical stability that increased with the size of the oligomeric structure.[43] In that particular approach, α-synuclein monomers were covalently linked into dimeric and tetrameric constructs by short peptide linkers. It remains to be studied how mechanical stability of a protein monomer is influenced by typical quaternary structures that are naturally and commonly formed
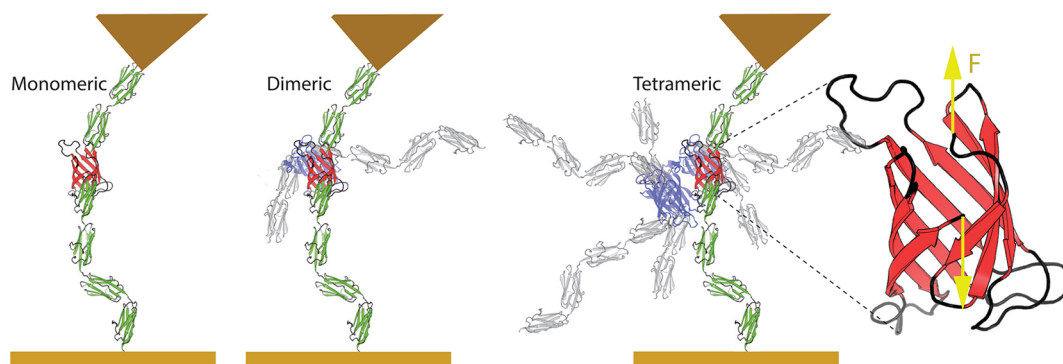
Figure 1. Schematic of a I27$_2$-SM-I27$_2$ AFM unfolding experiment. In each experiment, we pull directly on the monomer of Streptavidin (yellow arrows indicate forces). The pulling of a monomeric, dimeric, and tetrameric form is controlled through variants of the Streptavidin monomer (SM), which are always flanked by the I27 handles. In the dimeric and tetrameric pulling experiments, we still pull directly on a single monomer through I27 handles (green), while the handles from the multimerized molecule (gray) are not directly affecting the experiment.

through noncovalent interactions between participating monomers.

We chose Streptavidin (SA) as a model protein of multimerization. SA is normally a homo tetramer:[44] two SA monomers (SM) combine first to form a SA dimer, and then two SA dimers associate to form a tetramer. SA is a good model system because it has been extensively studied using a variety of chemical approaches including mutational analysis that identified critical mutations within the SA monomer to form only a dimer[45−47] or to stay monomeric.[48,49] These findings allow three forms of quaternary structure to be generated and tested by SMFS. Since the process of multimerization increases the thermal stability of SA tetramers,[48,50] we predict that it may also increase the mechanical stability (although the two are not always correlated[51,52]). Previously, the mechanical strength of various interfaces within SA tetramers was investigated with AFM, and the interface between two dimers was found to be significantly weaker as compared to the strength of the interface between two monomers.[39] These measurements were achieved by pulling on SA tetramers *via* polypeptide handles that were attached to different monomers within one dimer or monomers belonging to two different dimers.[39] In contrast, here we probe the mechanical unfolding pathways and the mechanical strength of SA monomer by directly pulling on its N- and C-termini through pulling handles, while allowing the monomer to engage in dimeric or tetrameric complexes (Figure 1). In each of our experiments, the unfolding reaction coordinate is defined by the direction and distance between the N and C termini, and the measurements are carried on SA monomers that are allowed to form on higher order oligomers or on various SA mutants that have a reduced ability to form oligomers.

SA has exceptionally high affinity for biotin,[53] and we use this ligand binding to obtain new information about how the ligand affects the strength of multimerization in SA. Because the biotin binding comes

from a loop donated across the interface between dimers (Supporting Information Figure S1), we hypothesize that biotin can only increase the mechanical stability in the unfolding pathway for SA that is able to form a tetramer rather than the event in which the formation of only a dimer or a monomer is possible. We can determine the extent to which the biotin binding stabilizes the complex by performing experiments with SA that has mutations to the critical residues.

RESULTS AND DISCUSSION

Streptavidin Monomers in Dimeric and Tetrameric Structures Have Increased Mechanical Strength. We first determined the strength of the monomeric Streptavidin monomer (SM$_{mon}$) using four mutations that stabilize SA in a monomeric form: V55T, T76R, L109T, and V125R. These mutations replace residues in the interface between the dimers and in the interface between the monomers with bulkier residues that prevents multimerization, but does not affect stability or the ability to bind biotin (though affinity is decreased).[49] SM$_{mon}$ was flanked by I27 domains and pulled using the I27 handles at constant velocity, as in Figure 1, with the ends of a single molecule tethered to both tip and substrate. Single-molecule events are readily distinguished from multiple-molecule events by recording five to six force peaks that report the unfolding of I27 domains and have normal contour-length increments of I27 domains.
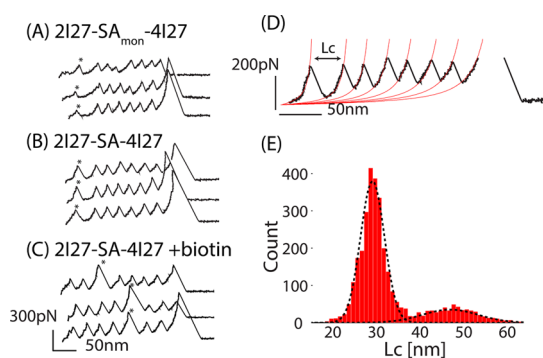
The normal unfolding force−extension trace of I27$_2$-SM$_{mon}$-I27$_4$ is shown in Figure 2A and Supporting Information Figure S2, which shows the unfolding of SM$_{mon}$ followed by the six I27 domains. The contour-length increments were measured for each peak and were fitted to two normal distributions at 29.2 ± 2.9 nm and at 47.1 ± 6.4 nm (Figure 2E). The protein I27 is expected to have an unfolding contour length increment of 28.7 nm,[14] which corresponds well with the measured 29.2 nm. A Streptavidin monomer has 132 residues and an initial length of 1.1 nm, and has a theoretical

contour-length increment of 47 nm (132 residues × 0.365 nm/residue[54] − 1.1 nm initial length), which corresponds well to the measured contour-length increment of 47.1 nm. The difference between contour-length increments between I27 domains and SM domains provides a simple way of distinguishing Streptavidin unfolding events from I27 unfolding events. The SM_{mon} unfolds at mean force of 109 ± 5 pN (mean ± SE; Figure 2, Supporting Information Figures S3 and S4; Table 1). The unfolding force of SM_{mon} is significantly lower than the unfolding force of I27 (199 ± 1 pN; mean ± SE; n = 969, Supporting Information Figure S5) and therefore appears first in the force−extension (FE) curve.[55]

We then characterized the mechanical strength of a monomer within the dimeric Streptavidin (SM_{dim}). The wildtype SA can be made dimeric using the single mutation W120 K, where the bulky lysine interferes with the interface between the dimers and prevents tetramerization.[46,47] The presence of I27 handles did not affect the dimerization of Streptavidin as confirmed by AFM imaging (Supporting Information Figure S6). The FE curves of $I27_2$-SM_{dim}-$I27_4$ are similar to the $I27_2$-SM_{mon}-$I27_4$ (Supporting Information Figure S2), except that the unfolding force of SM_{dim} is increased to 153 ± 7 pN (n = 54). Thus, the dimerization

Figure 2. Unfolding of the Streptavidin monomer (SM) flanked by I27 domains. (A−C) Typical unfolding patterns of Streptavidin monomer (marked by asterisk (*)), where (A) shows monomeric SM, (B) shows tetrameric SM, and (C) tetrameric SM with biotin. (D) Shows the fit of a worm-like chain (red) to the unfolding events and the contour length increment measurement, Lc, for a typical force−extension curve. (E) A histogram of all contour length increments shows two distributions, centered around 29.2 and at 47.1 nm, which correspond well to the theoretical contour length increment of I27 and Streptavidin, respectively.

increases the unfolding force of the SM by 40% (95% CI:[24, 56], p = 3 × 10⁻⁶). We then characterized the wildtype tetrameric Streptavidin monomer (SM_{wt}) which normally forms a highly stable tetramer[44] even when attached to polyI27 domains.[37,39] The flanking I27 domains in the $I27_2$-SM_{wt}-$I27_4$ construct did not disturb the tetramerization as confirmed by SDS-gel and AFM imaging (Supporting Information Figures S6 and S7); we expect that SM_{wt} will unfold while it is still tetramerized to the other $I27_2$-SM_{wt}-$I27_4$ constructs (Supporting Information Figure S8). The FE of $I27_2$-SM_{wt}-$I27_4$, shown in Figure 2(B), is also similar to $I27_2$-SM_{mon}-$I27_4$ except that the unfolding force of SM_{wt} has increased to 190 ± 5 pN (n = 211). This is an increase of 24% compared to the unfolding of SM_{dim} (95% CI:[10, 37], p = 7 × 10⁻⁴).

Simulated Unfolding Forces Correlate with Experimental Unfolding Forces for Different Multimeric States. We used coarse-grained steered molecular dynamic simulations to test our interpretation that the stabilization is provided through the interfaces generated by multimerization. We simulated the forced unfolding of a SA monomer coarse-grain model in monomeric, dimeric, and tetrameric Streptavidin (Materials and Methods). The simulated unfolding for the monomeric SM resulted in a single force peak (Supporting Information Figure S9, blue) similar to experiment. The peak involves the rupture of the two beta-strands, a strand at the N-terminus (residues 17−24) and a strand at the C-terminus (residues 122−130). The simulated unfolding of the dimer and tetramer also resulted in a first peak from the rupture of the N-terminal and C-terminal beta strands, however was followed by sequential unfolding of other strands which make intermolecular contacts. However, it is unlikely that the unfolding events after the first correlate with reality because the first unfolding event ruptures two beta strands on the outside of the barrel of Streptavidin. Like most proteins, Streptavidin contains the majority of its hydrophobic residues within the protein core (Supporting Information Figure S10) which protects these residues from the polar environment. However, in these coarse-grain simulations there is no solvent, so the interactions between hydrophobic residues and its environment are neglected. Thus, we compare only the forces of the first rupture peak in the simulation against the forces found in the experiments, in Figure 3A, which should still

TABLE 1. Summary of unfolding properties

	biotin log10 (K_a)	multimerization	F_{unf} − biotin mean ± SE (n)	F_{unf} + biotin mean ± SE (n)	% change [95% CI]	p-value
SM_{wt}	13.4[53]	Tet.[44]	190 ± 5 (211)	284 ± 5 (303)	+50[43,58]	10⁻³²
SM_{W120F}	11.7[56]	Tet.[45]	188 ± 6 (67)	293 ± 11 (52)	+56[42,70]	6 × 10⁻¹²
$SM_{W120A,K121A}$	7[a,57]	Tet.[a57]	180 ± 3 (35)	226 ± 8 (93)	+25[11,39]	5 × 10⁻⁴
SM_{dim}	7.2[46,47]	Dim.[46,47]	153 ± 7 (54)	169 ± 6 (71)	NC.	0.09
SM_{mon}	6.7[49]	Mon.[49]	109 ± 5 (53)	116 ± 4 (90)	NC.	0.4

[a] W120A,K121A used in this study, and the reference refers to W120A for reasons stated in the main text.
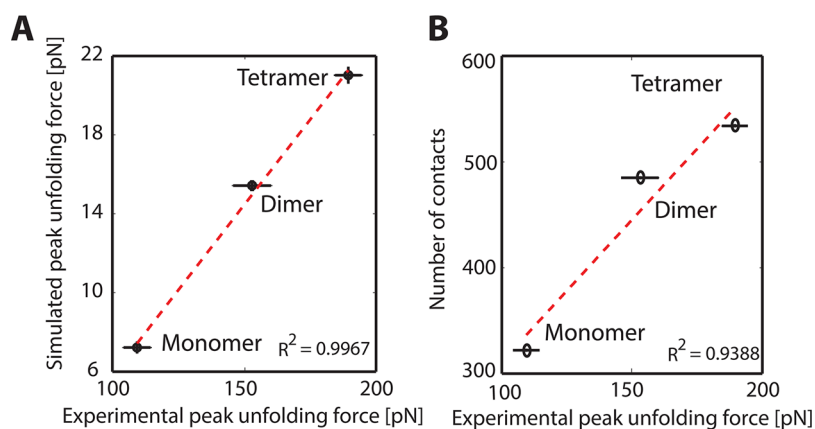
Figure 3. (A) Simulated peak unfolding force plotted against experimental unfolding forces with vertical and horizontal bars showing standard deviation of unfolding force (vertical too small to be seen). (B) Number of residue contacts available to a monomer within the multimeric states plotted against the experimental unfolding force.

approximate the effect of mechanical denaturation on a protein.

The unfolding forces between simulation and experimental correlate extremely well indicating that the stabilization is indeed due to the multimerization. Interestingly, there is also a high correlation between the number of contacts in a monomer/dimer/tetramer *versus* its unfolding force (Figure 3B). This has previously been found to be true for the unfolding forces of very homologous proteins,[58] and in general, it is true for proteins when they are normalized against the number of amino acids (comparing contact density).[59] However, to our knowledge, it has never been demonstrated for multimerization. This indicates that the unfolding force may be most dependent on only the organization and strength of contacts and that a coarse grain model may be a simple tool to calculate these and predict mechanical strength.

Biotin-Modulated Strengthening Requires Dimer−Dimer Interface from Tetrameric State. We also tested the unfolding pathways of SM_{wt}, SM_{dim}, and SM_{mon} in the presence of their cofactor, biotin (affinities in Table 1), to determine whether biotin binding would provide further strengthening and whether it would be dependent on the multimeric state. The crystal structure of Streptavidin[44] suggests that the loops of Streptavidin (residues 114−122) cross over the dimer−dimer interface to cap the biotin-binding pocket, ultimately forming favorable interactions between Trp120 and biotin (Supporting Information Figure S1). Since both SM_{dim} and SM_{mon} are missing a interface between the dimers, the extra stabilization provided through the biotin-loop interaction are absent, which would eliminate any further stabilization from biotin. Thus, we hypothesized that only tetrameric Streptavidin is strengthened by biotin binding. Indeed, the tetrameric SM_{wt} is greatly affected by biotin: the SM_{wt} unfolding force increases by 50% (Table 1), as shown in Figure 2C and Supporting Information Figure S2. The unfolding forces of both SM_{dim} and SM_{mon} are unaffected by

biotin (no change in unfolding force, $p = 0.09$ and $p = 0.4$, respectively, Table 1), which supports our hypothesis.

To verify whether the stabilization of the SM_{wt} with biotin is due to the binding loop, we tested the unfolding force of the monomer with mutations to critical residues in the binding loop. We first made the mutation W120F, which has been characterized to reduce the binding affinity by 2 orders of magnitude but does not affect tetramerization.[56] We found that the flanking I27 domains do not affect the tetramerization of SM_{W120F} (Supporting Information Figure S6) . The unfolding force of SM_{W120F} without biotin is indistinguishable from the wildtype SM_{wt} without biotin ($p = 0.9$), indicating that SM_{W120F} forms a tetramer similar to wildtype. Surprisingly, the unfolding force with biotin is also indistinguishable from wildtype SM_{wt} with biotin ($p = 0.5$), an indication that the phenylalanine can form a similar interaction as the tryptophan and can still provide considerable mechanical stability.

We then made a more severe double mutation to the biotin-binding loop using W120A and K121A ($SM_{W120A,K121A}$) mutations. The single-mutation W120A in SA has a substantial effect on biotin binding by reducing the association constant by 7 orders of magnitude although the protein remains as a tetramer.[57] We chose to test the double-mutation W120A and K121A instead of just the single-mutation W120A because the crystal structure of SA with W120A[60] shows that K121 can adopt a rotamer that forms favorable interactions with biotin, possibly alleviating the effects of W120A during mechanical unfolding (Supporting Information Figure S11). Since the single-mutation W120A still forms a tetramer, we expected the double mutant would also stay tetrameric, and this was confirmed by AFM imaging (Supporting Information Figure S6). Indeed, comparisons of the unfolding force without biotin for $SM_{W120A,K121A}$ is indistinguishable from the unfolding force for the tetrameric wildtype SM_{wt} without biotin ($p = 0.5$). However, the double mutant W120A-K121A mutation had a large effect on
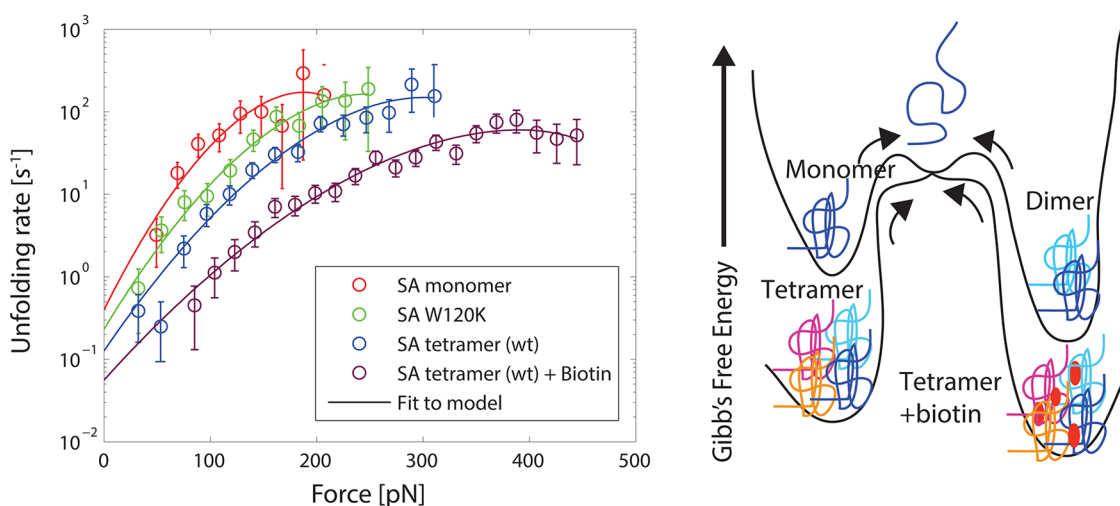
Figure 4. (Left) Unfolding rate-force map for variants of Streptavidin and fits associated with the one-dimensional diffusion over a barrier with applied force (see Materials and Methods). Unfolding rates generally decrease when going from monomeric to tetrameric, in line with what we observed for the effects on mechanical strengthening. (Right) Cartoon of the energy landscape showing that we are directly measuring the transition from the folded to unfolded state of a monomer in a protein of varying multimerization states.

TABLE 2. Summary of Fit Parameters[a]

Streptavidin state	intrinsic unfolding rate, K_{Unf} [s^{-1}]	distance to transition State, x_b [nn]	barrier height, G [K_BT]
Monomer	0.40 ± 0.30	0.26 ± 0.07	8.0 ± 1.1
Dimer	0.23 ± 0.09	0.21 ± 0.02	8.5 ± 0.4
Tetramer	0.13 ± 0.03	0.19 ± 0.01	9.0 ± 0.3
Tetramer +Biotin	0.06 ± 0.02	0.14 ± 0.01	8.9 ± 0.4
I27	$9.8 \pm 5.2 \times 10^{-4}$	0.31 ± 0.02	15.2 ± 0.4

[a] Values shown are best fit $\pm$ one standard deviation.

the unfolding force with biotin, as it resulted in a decrease in the unfolding force by 21% as compared to the wildtype with biotin (95% CI: [−28, −13], $p = 4 \times 10^{-8}$).

Increased Mechanical Stability Reflects Increased Folding Stability. The distribution of unfolding forces from SMFS experiments can be directly related to the unfolding rates to determine underlying energy landscape at zero force, as described previously.[61−65] Using these models, we determined the parameters of the energy landscape associated with the unfolding of Streptavidin along the N−C extension (see Materials and Methods for full description of analysis). The fits of this model are shown in Figure 4, and the parameters of this energy landscape (intrinsic unfolding rate, distance to transition state, and free energy) are shown in Table 2. The parameters for I27 were also determined and are comparable with previously determined parameters for I27 using this model.[61]

The relative unfolding rates correspond to the mechanical stabilities, as the unfolding rates decrease as the multimeric state increases. Interestingly, the cause of this decreasing unfolding rate seems to be due to a modest increase in barrier height (∼0.5 k_BT), as well as a slight decrease in the distance to the transition state with each increasing multimeric state. Thus, providing

multimerization not only increases the barrier height but also makes the energy well of the native state more narrow and thus creates a steeper barrier. We are further investigating the nature of these energy wells using all-atom explicit-solvent simulations.

It is worth noting that the unfolding rate of Streptavidin in the tetramer determined here (≈ 0.13 s^{-1}) differs by many orders of magnitude to the unfolding rate determined by chemical denaturation (≈ 2 × 10^{-8} s^{-1}).[66] The difference between these unfolding rates is likely due to the reaction coordinate under study; here we study the unfolding along the reaction coordinate defined by the N−C extension. In some cases, the unfolding rate determine along the N−C reaction coordinate is very similar to that obtained by chemical denaturation,[67] but this is protein-dependent and, in principle, may not be the same.[68]

CONCLUSIONS

The mechanical stability and unfolding rate of a protein monomer in a multimer is not as well understood as the mechanical stability and unfolding behavior of single-domain monomeric proteins. Here, we have shown the effect of multimerization on the mechanical unfolding pathway of Streptavidin (SA), and we find that there are substantial increases in

stability as the quaternary structure grows from monomer to dimer and to tetramer. Interestingly the simple increase of contacts caused by progression of quaternary structure had a high correlation to the mechanical stability (Figure 3).

The experimental unfolding force of the wildtype Streptavidin monomer increases 50% in the presence of biotin, which is similar to the increases seen in other protein—ligand complexes (typically 40—120%).[59] This increased strength is likely due to the biotin-binding loop that bridges the dimer—dimer interface and is supported by our observations that the unfolding forces of SM_{dim} and SM_{mon} (both devoid of a interface between dimers) are unaffected by biotin. Also, the strengthening of the biotin binding loop is supported by our observation that the unfolding force of the $SM_{W120A,K121A}$, which carries a mutated biotin-binding loop, was considerably weaker than that of the wild-type. Interestingly, unlike other studied protein—ligand complexes that strengthen the mechanical stability of a single monomer, the biotin ligand in Streptavidin is an intermolecular strengthening provided only when the Streptavidin dimers are associated into their tetrameric structure.

These results provide direct evidence that multimerization not only provides significant mechanical folding stability due to the neighboring interfaces but also provides additional strengthening mechanisms through ligand-multimer interactions. These findings are important for understanding the stability of protein complexes in the cell and for designing novel multimeric proteins for the development of new biomaterials and drug delivery systems.

MATERIALS AND METHODS

Protein Engineering. To perform pulling experiments, we flanked the protein Streptavidin monomer (SM) by I27 protein domains at the DNA level. The addition of I27 domains as handles facilitates the pickup of the molecule and they serve as a positive control and fingerprint of a single molecule event.[69] The final construct is composed of two I27 domains, the Streptavidin domain, and four I27 domains, each connected with short two amino acid linkers ($I27_2$-SM-$I27_4$). This construct was obtained from replacing the third and fourth modules of the poly(I27) pRSETa vector, a kind gift from Jane Clarke,[70] with Streptavidin monomer.

Variants for Streptavidin were made by directly mutating the wildtype SM or synthesized directly and reinserted into the poly(I27) pRSETa vector. The variants include the following: (1) W120F; (2) W120K (denoted SM_{dim} because it forms dimeric SA); (3) W120A and K121A; and (4) V55T, T76R, L109T, and V125R (denoted SM_{mon} because it forms monomeric SA). All engineered plasmids were transformed into *Escherichia coli* C41(DE3)pLysS cells, and expression was induced using IPTG. Cell lysate was run through a Ni-NTA column (Qiagen, Valencia, CA) and the protein was collected and stored in 40% glycerol and 60% PBS pH 7.4 at −20 °C. The eluted wildtype SA ($I27_2$-SM_{wt}-$I27_4$) was analyzed by SDS-gel (Supporting Information Figure S7) and found to be similar to previous SA-I27 chimeras,[37,39] which supports our hypothesis that tetramerization is not affected by the flanking I27 domains. To further validate this conclusion, we directly determined the multimerization state using AFM Imaging S6.

AFM Spectroscopy. All AFM measurements were obtained using a custom-built AFM instrument.[20] Automation routines to control the AFM[71] were implemented in Labview 7.0 (National Instruments, Austin, TX). Cantilever spring constants were calibrated in the buffer solution using the energy equipartition theorem.[72] All measurements were done at a constant velocity of 300 nm/s, in a PBS pH 7.4 solution at room temperature or PBS pH 7.4 with 2 mM biotin (when specified). In all experiments, the purified protein was diluted to 150 μg/mL, and applied to recently evaporated gold and incubated for 1 h. Measurements were performed using MLCT cantilevers (Bruker, Camarillo, CA) which have a spring constant of 16 ± 3 pN/nm.

A worm-like chain (WLC) model with persistence of 0.4 nm was fit to each peak in order to measure contour length increments in the force—extension (FE) data.[73] The contour-length increments from every peak in every recording were fit using a mixture model with two distributions (for I27 domains and Streptavidin domains) (Figure 2E). The 95% confidence intervals for the contour length increments of the two distributions were used for labeling an unfolding event as I27 (23.5—34.6 nm) or labeling an unfolding event as unfolding of Streptavidin monomer (34.6—59.6 nm) in order to eliminate human-bias in data selection.

Statistical Analysis. The unfolding forces were compared statistically, using a total of 15 tests (comparing to wildtype, comparing between ligand-bound and apo, *etc.*). For statistical significance, then, we used a Bonferroni corrected *p*-value of $0.05/15 = 0.0033$. Comparisons were made using a two-sample *t* test with null hypothesis that both distributions are normal with the same means. The assumption of equal variances in the two-sample *t* test was used only if null hypothesis of the two-sample F-test that the variances are equal could not be rejected. The assumption of normality for the distributions is also valid when doing the two-sample *t* test because the null hypothesis that the data comes from a normal could not be rejected when subjected to the one-sample Kolmogorov—Smirnov test (Supporting Information Figure S12).

Coarse-Grain Simulation. Structure based models were generated using the SMOG web server[74] from PDB 1SWE.[75] In this coarse-grain model, each residue is modeled as a single pseudo-atom. Steered molecular dynamics are conducted on this model with the forces determined by a coarse-grain potential. This potential contains terms for bonds, angles, and improper angles, which have equilibrium values based on the initial structure. All residues identified as a contact have an attractive 12—6 potential and residues identified as noncontacts have a repulsive 12 potential. More information about parameter values are described by Clementi *et al.*[76] The temperature used for all calculations was the folding temperature at which the folded state and the unfolded state of the monomeric Streptavidin are equally populated. The folding temperature was found by determining where the specific heat is maximal (Supporting Information Figure S13). Simulations were conducted using GROMACS 4.5.5[77] by pulling on the N-terminus with reference to the C-terminus, at 0.1 nm/ns and using spring constant of 6 pN/nm. The pulling geometry was the same for the monomer, dimer, and tetramer form of Streptavidin. Examples of force—extension traces are shown in Supporting Information Figure S9. We conducted 8—20 simulations for each type of Streptavidin experiment to estimate the mean simulated peak unfolding force.

Modeling Unfolding. The process of unfolding of a protein along the N—C extension reaction coordinate can be thought of as rate of escape over a barrier for a process that undergoes one-dimensional diffusion, where the force applied enters as a linear potential that modulates the height of the barrier. Previous work by Dudko *et al.*[61,62] provide the framework for this analysis

that allows for extracting parameters of the energy landscape at zero force from distributions of unfolding forces. The model used in this paper comes from Dudko et al.:[61]

$$k(f) = k_0 \left(1 - \frac{\nu f x_b}{\Delta G}\right)^{1/\nu - 1} \exp\left(\frac{\Delta G}{k_B T}\left[1 - \left(1 - \frac{\nu f x_b}{\Delta G}\right)^{1/\nu}\right]\right) \tag{1}$$

where ν is a general parameter that adjusts for the shape of the barrier ($\nu = 1/2$ used here to model a harmonic-cusp potential), x_b is the distance from the well minimum to the barrier (distance to transition state), ΔG is the barrier height, and k_0 is the intrinsic unfolding rate (at zero force).

This model requires knowing the unfolding rate at a given force, $k(f)$. By assuming that the unfolding is a Markovian process, the force-dependent unfolding rate can be readily determined from force-distributions and is given by the following equation, derived by Evans et al.[63] and Zhang and Dudko:[65]

$$k(F_k) = \frac{\Delta N_{unf}(k) \cdot r(F_k)}{\Delta F \cdot N_{folded}(F_k)} \tag{2}$$

The k subscript here represents a bin in the histogram of forces, $\Delta N_{unf}(k)$ represents the number of events in bin k, ΔF is the bin size, $N_{folded}(F_k)$ is the total number of events still folded at force F_k, and $r(F_k)$ is the loading rate calculated at that force. Errors associated with using a given bin size of the histogram can also be estimated as from Zhang and Dudko[65] as

$$\sigma_{\ln k(f)} \approx \left[\frac{1}{\Delta N_{unf}(k)} + \frac{1}{N_{folded}(F_k)}\right] \tag{3}$$

The loading rate can be calculated two ways: by simply taking the slope right before the force-rupture of the force vs time plot (as in Zhang and Dudko[65]) or by using a highly accurate approximation of the loading rate using a worm-like chain interpolation formula (as in Dudko et al.[62]):

$$r(F) = V\left[\frac{1}{K_{AFM}} + \frac{2L_c b(1 + Fb)}{3 + 5Fb + 8(Fb)^{5/2}}\right]^{-1} \tag{4}$$

where V is the speed, K_{AFM} is the cantilever stiffness, L_c is the contour length, and $b = p/k_B T$ where p is the persistence length. In this study, we used the interpolation formula; however, we obtained similar results with both methods.

For fitting our data, we first extracted the force-dependent unfolding rates using eqs 2 and eq 4 and determined their associated errors. We then performed a nonlinear regression using Matlab (nlinfit) using the force-dependent unfolding rates and eq 1 and obtained confidence intervals for one standard deviation. As a control, we included analysis of the I27 unfolding events in the table which are very close to what has been previously reported for I27 using this model.[61]

AFM Imaging. AFM images were taken using a Nanoscope V MultiMode scanning probe microscope (Veeco Instruments, Plainview, NY) using AFM and LFM mode. Samples were prepared by depositing 1−5 nM protein onto freshly cleaved mica for 5−10 s before washing gently with water and drying with filtered air. All measurements were done in air using a single RTESPA probe (Bruker, Billerica, MA), which had a resonance frequency of 305.5 kHz. Images were collected at a scan rate of 2.0 Hz with a a scan resolution of 512 × 512 pixels, and a scan size of 2800 nm. In each experiment, 8−10 images were captured and 200−300 proteins total were analyzed.

Image analysis was done by first flattening the image using the Nanoscope 7.3 software. Images were then imported into Gwyddion[78] for subsequent analysis. The particles in each image were masked in order to calculate the volume. The selection of individual particles to mask was done blindly, by a person not familiar with the experiment who also had no knowledge of the type of particle in any image. This control allows the selection step to be done without introducing subjective bias. The volume was then calculated for each masked particle using the grain minimum basis volume to account for local background. Example of images and the

evaluated mean volume is shown in Supporting Information Figure S6. These volumes correspond well to the known multi-merization state of each protein.

Conflict of Interest: The authors declare no competing financial interest.

Supporting Information Available: Protein sequences of constructs used in this study; cartoon of dimer-dimer interaction from PDB 1SWE ; examples of the force-extension curves for unfolding SM$_{mon}$, SM$_{dim}$, and SM$_{wt}$ with and without Biotin; box and whisker plots for unfolding forces of each construct; distributions of unfolding forces of each construct; comparison of distributions between different experiments; AFM images confirming correct multimerization; SDS-gel of the Streptavidin constructs; cartoon of the multiple-attachment that leads to unfolding events; force-extension curves from coarse-grain simulations of Streptavidin unfolding; polar and hydrophobic residues of Streptavidin monomer; structure of Streptavidin mutants biotin-binding pocket; statistical tests for normality of unfolding distributions; specific heat calculations for simulations of the coarse-grain model of the Streptavidin monomer; anisotropy of SA peaks during unfolding of tetrameric structure. This material is available free of charge via the Internet at http://pubs.acs.org.

REFERENCES AND NOTES

1. Braselmann, E.; Chaney, J. L.; Clark, P. L. Folding the Proteome. *Trends Biochem. Sci.* **2013**, *38*, 337–344.

2. Matsumoto, M.; Hwang, S. B.; Jeng, K.-S.; Zhu, N.; Lai, M. Homotypic Interaction and Multimerization of Hepatitis C Virus Core Protein. *Virology* **1996**, *218*, 43–51.

3. Lv, S.; Dudek, D. M.; Cao, Y.; Balamurali, M. M.; Gosline, J.; Li, H. Designed Biomaterials to Mimic the Mechanical Properties of Muscles. *Nature* **2010**, *465*, 69–7310.1038/nature09024.

4. Langer, R.; Tirrell, D. A. Designing Materials for Biology and Medicine. *Nature* **2004**, *428*, 487–492.

5. Douglas, T.; Young, M. Host-Guest Encapsulation of Materials by Assembled Virus Protein Cages. *Nature* **1998**, *393*, 152–155.

6. Neuman, K. C.; Nagy, A. Single-Molecule Force Spectroscopy: Optical Tweezers, Magnetic Tweezers and Atomic Force Microscopy. *Nat. Methods* **2008**, *5*, 491–505.

7. Borgia, A.; Williams, P. M.; Clarke, J. Single-Molecule Studies of Protein Folding. *Annu. Rev. Biochem.* **2008**, *77*, 101–125.

8. Hoffmann, t.; Dougan, L. Single Molecule Force Spectroscopy Using Polyproteins. *Chem. Soc. Rev.* **2012**, *41*, 4781–4796.

9. Noy, A.; Friddle, R. W. Practical Single Molecule Force Spectroscopy: How to Determine Fundamental Thermodynamic Parameters of Intermolecular Bonds with an Atomic Force Microscope. *Methods* **2013**, *60*, 142–150.

10. Žoldák, G.; Rief, M. Force as a Single Molecule Probe of Multidimensional Protein Energy Landscapes. *Curr. Opin. Struct. Biol.* **2013**, *23*, 48–57.

11. Woodside, M.; Block, S. Reconstructing Folding Energy Landscapes by Single-Molecule Force Spectroscopy. *Annu. Rev. Biophys.* **2014**, *43*, 19.

12. Rief, M.; Gautel, M.; Oesterhelt, F.; Fernandez, J. M.; Gaub, H. E. Reversible Unfolding of Individual Titin Immunoglobulin Domains by AFM. *Science* **1997**, *276*, 1109–1112.

13. Oberhauser, A. F.; Marszalek, P. E.; Erickson, H. P.; Fernandez, J. M. The Molecular Elasticity of the Extracellular Matrix Protein Tenascin. *Nature* **1998**, *393*, 181–185.

14. Carrion-Vazquez, M.; Oberhauser, A. F.; Fowler, S. B.; Marszalek, P. E.; Broedel, S. E.; Clarke, J.; Fernandez, J. M. Mechanical and

Chemical Unfolding of a Single Protein: A Comparison. *Proc. Natl. Acad. Sci. U.S.A.* **1999**, *96*, 3694–3699.

15. Viani, M. B.; Schaffer, T. E.; Chand, A.; Rief, M.; Gaub, H. E.; Hansma, P. K. Small Cantilevers for Force Spectroscopy of Single Molecules. *J. Appl. Phys.* **1999**, *86*, 2258–2262.

16. Oberhauser, A. F.; Hansma, P. K.; Carrion-Vazquez, M.; Fernandez, J. M. Stepwise Unfolding of Titin Under Force-Clamp Atomic Force Microscopy. *Proc. Natl. Acad. Sci. U.S.A.* **2001**, *98*, 468–472.

17. Williams, P. M.; Fowler, S. B.; Best, R. B.; toca Herrera, J. L.; Scott, K. A.; Steward, A.; Clarke, J. Hidden Complexity in the Mechanical Properties of Titin. *Nature* **2003**, *422*, 446–449.

18. Fernandez, J. M.; Li, H. Force-Clamp Spectroscopy Monitors the Folding Trajectory of a Single Protein. *Science* **2004**, *303*, 1674–1678.

19. Gutsmann, T.; Fantner, G. E.; Kindt, J. H.; Venturoni, M.; Danielsen, S.; Hansma, P. K. Force Spectroscopy of Collagen Fibers To Investigate Their Mechanical Properties and Structural Organization. *Biophys. J.* **2004**, *86*, 3186–93.

20. Lee, G.; Abdi, K.; Jiang, Y.; Michaely, P.; Bennett, V.; Marszalek, P. E. Nanospring Behaviour of Ankyrin Repeats. *Nature* **2006**, *440*, 246–249.

21. Bornschlog, T.; Rief, M. Single-Molecule Dynamics of Mechanical Coiled-Coil Unzipping. *Langmuir* **2008**, *24*, 1338–1342.

22. Dietz, H.; Berkemeier, F.; Bertz, M.; Rief, M. Anisotropic Deformation Response of Single Protein Molecules. *Proc. Natl. Acad. Sci. U.S.A.* **2006**, *103*, 12724–12728.

23. Kessler, M.; Gottschalk, K. E.; Janovjak, H.; Muller, D. J.; Gaub, H. E. Bacteriorhodopsin Folds into the Membrane against an External Force. *J. Mol. Biol.* **2006**, *357*, 644–654.

24. Junker, J. P.; Rief, M. Single-Molecule Force Spectroscopy Distinguishes Target Binding Modes of Calmodulin. *Proc. Natl. Acad. Sci. U.S.A.* **2009**, *106*, 14361–14366.

25. Lee, W.; Zeng, X.; Zhou, H.-X.; Bennett, V.; Yang, W.; Marszalek, P. E. Full Reconstruction of a Vectorial Protein Folding Pathway by Atomic Force Microscopy and Molecular Dynamics Simulations. *J. Biol. Chem.* **2010**, *285*, 38167–38172.

26. Ainavarapu, S. R. K.; Li, L. Y.; Badilla, C. L.; Fernandez, J. M. Ligand Binding Modulates the Mechanical Stability of Dihydrofolate Reductase. *Biophys. J.* **2005**, *89*, 3337–3344.

27. Junker, J. P.; Ziegler, F.; Rief, M. Ligand-Dependent Equilibrium Fluctuations of Single Calmodulin Molecules. *Science* **2009**, *323*, 633–637.

28. Cao, Y.; Kuske, R.; Li, H. Direct Observation of Markovian Behavior of the Mechanical Unfolding of Individual Proteins. *Biophys. J.* **2008**, *95*, 782–788.

29. Wang, C.-C.; Tsong, T.-Y.; Hsu, Y.-H.; Marszalek, P. E. Inhibitor Binding Increases the Mechanical Stability of Staphylococcal Nuclease. *Biophys. J.* **2011**, *100*, 1094–1099.

30. Florin, E. L.; Moy, V. T.; Gaub, H. E. Adhesion Forces Between Individual Ligand-Receptor Pairs. *Science* **1994**, *264*, 415–417.

31. Moy, V. T.; Florin, E. L.; Gaub, H. E. Intermolecular Forces and Energies between Ligands and Receptors. *Science* **1994**, *266*, 257–259.

32. Fritz, J.; Katopodis, A. G.; Kolbinger, F.; Anselmetti, D. Force-Mediated Kinetics of Single P-selectin/Ligand Complexes Observed by Atomic Force Microscopy. *Proc. Natl. Acad. Sci. U.S.A.* **1998**, *95*, 12283–12288.

33. Evans, E. Looking Inside Molecular Bonds at Biological Interfaces with Dynamic Force Spectroscopy. *Biophys. Chem.* **1999**, *82*, 83–97.

34. Harada, Y.; Kuroda, M.; Ishida, A. Specific and Quantized Antigenantibody Interaction Measured by Atomic Force Microscopy. *Langmuir* **1999**, *16*, 708–715.

35. Merkel, R.; Nassoy, P.; Leung, A.; Ritchie, K.; Evans, E. Energy Landscapes of Receptor-ligand Bonds Explored with Dynamic Force Spectroscopy. *Nature* **1999**, *397*, 50–3.

36. Hinterdorfer, P.; Dufrne, Y. F. Detection and Localization of Single Molecular Recognition Events Using Atomic Force Microscopy. *Nat. Methods* **2006**, *3*, 347–355.

37. Kim, M.; Wang, C.-C.; Benedetti, F.; Marszalek, P. E. A Nanoscale Force Probe for Gauging Intermolecular Interactions. *Angew. Chem., Int. Ed.* **2012**, *51*, 1903–1906.

38. Kaur, P.; Qiang, F.; Fuhrmann, A.; Ros, R.; Kutner, L. O.; Schneeweis, L. A.; Navoa, R.; Steger, K.; Xie, L.; Yonan, C.; et al. Antibody-Unfolding and Metastable-State Binding in Force Spectroscopy and Recognition Imaging. *Biophys. J.* **2011**, *100*, 243–50.

39. Kim, M.; Wang, C.-C.; Benedetti, F.; Rabbi, M.; Bennett, V.; Marszalek, P. E. Nanomechanics of Streptavidin Hubs for Molecular Materials. *Adv. Mater.* **2011**, *23*, 5684–5688.

40. Yu, J.; Malkova, S.; Lyubchenko, Y. L. α-Synuclein Misfolding: Single Molecule AFM Force Spectroscopy Study. *J. Mol. Biol.* **2008**, *384*, 992–1001.

41. Hoffmann, A.; Neupane, K.; Woodside, M. T. Single-Molecule Assays for Investigating Protein Misfolding and Aggregation. *Phys. Chem. Chem. Phys.* **2013**, *15*, 7934–7948.

42. McAllister, C.; Karymov, M. A.; Kawano, Y.; Lushnikov, A. Y.; Mikheikin, A.; Uversky, V. N.; Lyubchenko, Y. L. Protein Interactions and Misfolding Analyzed by AFM Force Spectroscopy. *J. Mol. Biol.* **2005**, *354*, 1028–1042.

43. Neupane, K.; Solanki, A.; Sosova, I.; Belov, M.; Woodside, M. T. Diverse Metastable Structures Formed by Small Oligomers of α-Synuclein Probed by Force Spectroscopy. *PLoS One* **2014**, *9*, e86495.

44. Hendrickson, W. A.; Pähler, A.; Smith, J. L.; Satow, Y.; Merritt, E. A.; Phizackerley, R. P. Crystal Structure of Core Streptavidin Determined from Multiwavelength Anomalous Diffraction of Synchrotron Radiation. *Proc. Natl. Acad. Sci. U.S.A.* **1989**, *86*, 2190–2194.

45. Sano, T.; Cantor, C. R. Intersubunit Contacts Made by Tryptophan 120 with Biotin Are Essential for Both Strong Biotin Binding and Biotin-Induced Tighter Subunit Association of Streptavidin. *Proc. Natl. Acad. Sci. U.S.A.* **1995**, *92*, 3180–3184.

46. Pazy, Y.; Eisenberg-Domovich, Y.; Laitinen, O. H.; Kulomaa, M. S.; Bayer, E. A.; Wilchek, M.; Livnah, O. Dimer-Tetramer Transition between Solution and Crystalline States of Streptavidin and Avidin Mutants. *J. Bacteriol.* **2003**, *185*, 4050–4056.

47. Laitinen, O. H.; Airenne, K. J.; Marttila, A. T.; Kulik, T.; Porkka, E.; Bayer, E. A.; Wilchek, M.; Kulomaa, M. S. Mutation of a Critical Tryptophan to Lysine in Avidin or Streptavidin May Explain Why Sea Urchin Fibropellin Adopts an Avidin-like Domain. *FEBS Lett.* **1999**, *461*, 52–58.

48. Lim, K. H.; Huang, H.; Pralle, A.; Park, S. Engineered Streptavidin Monomer and Dimer with Improved Stability and Function. *Biochemistry* **2011**, *50*, 8682–8691.

49. Wu, S.-C.; Wong, S.-L. Engineering Soluble Monomeric Streptavidin with Reversible Biotin Binding Capability. *J. Biol. Chem.* **2005**, *280*, 23225–23231.

50. González, M.; Bagatolli, L. A.; Echabe, I.; Arrondo, J. L.; Argaraña, C. E.; Cantor, C. R.; Fidelio, G. D. Interaction of Biotin with Streptavidin Thermostability and Conformational Changes upon Binding. *J. Biol. Chem.* **1997**, *272*, 11288–11294.

51. Brockwell, D. J.; Paci, E.; Zinober, R. C.; Beddard, G. S.; Olmsted, P. D.; Smith, D. A.; Perham, R. N.; Radford, S. E. Pulling Geometry Defines the Mechanical Resistance of a Beta-Sheet Protein. *Nat. Struct. Biol.* **2003**, *10*, 731–7.

52. Paci, E.; Karplus, M. Unfolding Proteins by External Forces and Temperature: The Importance of Topology and Energetics. *Proc. Natl. Acad. Sci. U.S.A.* **2000**, *97*, 6521–6526.

53. Weber, P. C.; Ohlendorf, D.; Wendoloski, J.; Salemme, F. Structural Origins of High-Affinity Biotin Binding to Streptavidin. *Science* **1989**, *243*, 85–88.

54. Dietz, H.; Rief, M. Protein Structure by Mechanical Triangulation. *Proc. Natl. Acad. Sci. U.S.A.* **2006**, *103*, 1244–1247.

55. Li, H.; Oberhauser, A. F.; Fowler, S. B.; Clarke, J.; Fernandez, J. M. Atomic Force Microscopy Reveals the Mechanical Design of a Modular Protein. *Proc. Natl. Acad. Sci. U. S. A.* **2000**, *97*, 6527–6531.

56. Chilkoti, A.; Stayton, P. S. Molecular Origins of the Slow Streptavidin-Biotin Dissociation Kinetics. *J. Am. Chem. Soc.* **1995**, *117*, 10622–10628.

57. Chilkoti, A.; Schwartz, B. L.; Smith, R. D.; Long, C. J.; Stayton, P. S. Engineered Chimeric Streptavidin Tetramers as Novel

Tools for Bioseparations and Drug Delivery. *Nat. Biotechnol.* **1995**, *13*, 1198–1204.

58. Kotamarthi, H. C.; Sharma, R.; Koti Ainavarapu, S. R. Single-Molecule Studies on Polysumo Proteins Reveal Their Mechanical Flexibility. *Biophys. J.* **2013**, *104*, 2273–2281.

59. Li, Q.; Scholl, Z.; Marszalek, P. *Nanomech. Single Biomacromol.* **2014**, 1077–1123.

60. Freitag, S.; Le Trong, I.; Chilkoti, A.; Klumb, L. A.; Stayton, P. S.; Stenkamp, R. E. Structural Studies of Binding Site Tryptophan Mutants in the High-Affinity Streptavidin-Biotin Complex. *J. Mol. Biol.* **1998**, *279*, 211–221.

61. Dudko, O. K.; Hummer, G.; Szabo, A. Intrinsic Rates and Activation Free Energies from Single-Molecule Pulling Experiments. *Phys. Rev. Lett.* **2006**, *96*.

62. Dudko, O. K.; Hummer, G.; Szabo, A. Theory, Analysis, and Interpretation of Single-Molecule Force Spectroscopy Experiments. *Proc. Natl. Acad. Sci. U.S.A.* **2008**, *105*, 15755–15760.

63. Evans, E.; Halvorsen, K.; Kinoshita, K.; Wong, W. P. *Handbook of Single-Molecule Biophysics*; Springer: New York, 2009; pp 571–589.

64. Yu, H.; Liu, X.; Neupane, K.; Gupta, A. N.; Brigley, A. M.; Solanki, A.; Sosova, I.; Woodside, M. T. Direct Observation of Multiple Misfolding Pathways in a Single Prion Protein Molecule. *Proc. Natl. Acad. Sci. U.S.A.* **2012**, *109*, 5283–5288.

65. Zhang, Y.; Dudko, O. K. A Transformation for the Mechanical Fingerprints of Complex Biomolecular Interactions. *Proc. Natl. Acad. Sci. U.S.A.* **2013**, *110*, 16432–16437.

66. Kurzban, G.; Bayer, E.; Wilchek, M.; Horowitz, P. The Quaternary Structure of Streptavidin in Urea. *J. Biol. Chem.* **1991**, *266*, 14470–14477.

67. Carrion-Vazquez, M.; Oberhauser, A. F.; Fowler, S. B.; Marszalek, P. E.; Broedel, S. E.; Clarke, J.; Fernandez, J. M. AFM and Chemical Unfolding of a Single Protein Follow the Same Pathway. *Biophys. J.* **1999**, *76*, A173–A173.

68. Stirnemann, G.; Kang, S.-g.; Zhou, R.; Berne, B. J. How Force Unfolding Differs from Chemical Denaturation. *Proc. Natl. Acad. Sci. U.S.A.* **2014**, *111*, 3413–3418.

69. Scholl, Z. N.; Li, Q.; Marszalek, P. E. Single Molecule Mechanical Manipulation for Studying Biological Properties of Proteins, DNA, and Sugars. *Wiley Interdiscip. Rev.: Nanomed. Nanobiotechnol.* **2014**, *6*, 211–229.

70. Steward, A.; toca Herrera, J. L.; Clarke, J. Versatile Cloning System for Construction of Multimeric Proteins for Use in Atomic Force Microscopy. *Protein Sci.* **2002**, *11*, 2179–2183.

71. Scholl, Z. N.; Marszalek, P. E. improving Single Molecule Force Spectroscopy Through Automated Real-Time Data Collection and Quantification of Experimental Conditions. *Ultramicroscopy* **2014**, *136*, 7–14.

72. Florin, E. L.; Rief, M.; Lehmann, H.; Ludwig, M.; Dornmair, C.; Moy, V. T.; Gaub, H. E. Sensing Specific Molecular-Interactions with the Atomic-Force Microscope. *Biosens. Bioelectron.* **1995**, *10*, 895–901.

73. Marko, J. F.; Siggia, E. D. Stretching DNA. *Macromolecules* **1995**, *28*, 8759–8770.

74. Noel, J. K.; Whitford, P. C.; Sanbonmatsu, K. Y.; Onuchic, J. N. Smog@ Ctbp: Simplified Deployment of Structure-Based Models in Gromacs. *Nucleic Acids Res.* **2010**, *38*, W657–W661.

75. Stenkamp, R. E.; Trong, I. L.; Klumb, L.; Stayton, P. S.; Freitag, S. Structural Studies of the Streptavidin Binding Loop. *Protein Sci.* **1997**, *6*, 1157–1166.

76. Clementi, C.; Nymeyer, H.; Onuchic, J. N. topological and Energetic Factors: What Determines the Structural Details of the Transition State Ensemble and "En–Route" Intermediates for Protein Folding? an Investigation for Small Globular Proteins. *J. Mol. Biol.* **2000**, *298*, 937–95310.1006/jmbi.2000.3693.

77. Pronk, S.; Páll, S.; Schulz, R.; Larsson, P.; Bjelkmar, P.; Apostolov, R.; Shirts, M. R.; Smith, J. C.; Kasson, P. M.; van der Spoel, D.; et al. Gromacs 4.5: A High-Throughput and Highly Parallel Open Source Molecular Simulation Toolkit. *Bioinformatics* **2013**, btt055.

78. Neas, D.; Klapetek, P. Gwyddion: An Open-Source Software for SPM Data Analysis. *Cent. Eur. J. Phys.* **2012**, *10*, 181–188.